


# Impaired TFEB activation and mitophagy as a cause of PPP3/calcineurin inhibitor-induced pancreatic $\beta$ -cell dysfunction

Kihyoun Park, Seong Keun Sonn, Seungwoon Seo, Jinyoung Kim, Kyu Yeon Hur, Goo Taeg Oh & Myung-Shik Lee


To cite this article: Kihyoun Park, Seong Keun Sonn, Seungwoon Seo, Jinyoung Kim, Kyu Yeon Hur, Goo Taeg Oh & Myung-Shik Lee (2023) Impaired TFEB activation and mitophagy as a cause of PPP3/calcineurin inhibitor-induced pancreatic  $\beta$ -cell dysfunction, *Autophagy*, 19:5, 1444-1458, DOI: [10.1080/15548627.2022.2132686](https://doi.org/10.1080/15548627.2022.2132686)

To link to this article: <https://doi.org/10.1080/15548627.2022.2132686>

 View supplementary material 

 Published online: 10 Oct 2022.

 Submit your article to this journal 

 Article views: 1202

 View related articles 

 View Crossmark data 

RESEARCH PAPER



## Impaired TFEB activation and mitophagy as a cause of PPP3/calcineurin inhibitor-induced pancreatic $\beta$ -cell dysfunction

Kihyoun Park <sup>a,\*</sup>, Seong Keun Sonn <sup>b,\*</sup>, Seungwoon Seo <sup>b</sup>, Jinyoung Kim <sup>a</sup>, Kyu Yeon Hur<sup>c</sup>, Goo Taeg Oh <sup>b</sup>, and Myung-Shik Lee <sup>a,d</sup>

<sup>a</sup>Severance Biomedical Science Institute, Yonsei University College of Medicine, Seoul, Korea; <sup>b</sup>Heart-Immune-Brain Network Research Center, Department of Life Science, Ewha Womans University, Seoul, Korea; <sup>c</sup>Department of Medicine, Samsung Medical Center, Sungkyunkwan University School of Medicine, Seoul, Korea; <sup>d</sup>Soonchunhyang Institute of Medi-bio Science and Division of Endocrinology, Department of Internal Medicine, Soonchunhyang University College of Medicine, Cheonan, Korea

### ABSTRACT

Macroautophagy/autophagy or mitophagy plays crucial roles in the maintenance of pancreatic  $\beta$ -cell function. PPP3/calcineurin can modulate the activity of TFEB, a master regulator of lysosomal biogenesis and autophagy gene expression, through dephosphorylation. We studied whether PPP3/calcineurin inhibitors can affect the mitophagy of pancreatic  $\beta$ -cells and pancreatic  $\beta$ -cell function employing FK506, an immunosuppressive drug against graft rejection. FK506 suppressed rotenone- or oligomycin+antimycin-A-induced mitophagy measured by Mito-Keima localization in acidic lysosomes or RFP-LC3 puncta colocalized with TOMM20 in INS-1 insulinoma cells. FK506 diminished nuclear translocation of TFEB after treatment with rotenone or oligomycin+antimycin A. Forced TFEB nuclear translocation by a constitutively active TFEB mutant transfection restored impaired mitophagy by FK506, suggesting the role of decreased TFEB nuclear translocation in FK506-mediated mitophagy impairment. Probably due to reduced mitophagy, recovery of mitochondrial potential or quenching of mitochondrial ROS after removal of rotenone or oligomycin+antimycin A was delayed by FK506. Mitochondrial oxygen consumption was reduced by FK506, indicating reduced mitochondrial function by FK506. Likely due to mitochondrial dysfunction, insulin release from INS-1 cells was reduced by FK506 in vitro. FK506 treatment also reduced insulin release and impaired glucose tolerance in vivo, which was associated with decreased mitophagy and mitochondrial COX activity in pancreatic islets. FK506-induced mitochondrial dysfunction and glucose intolerance were ameliorated by an autophagy enhancer activating TFEB. These results suggest that diminished mitophagy and consequent mitochondrial dysfunction of pancreatic  $\beta$ -cells contribute to FK506-induced  $\beta$ -cell dysfunction or glucose intolerance, and autophagy enhancement could be a therapeutic modality against post-transplantation diabetes mellitus caused by PPP3/calcineurin inhibitors.

### ARTICLE HISTORY

Received 16 February 2022  
Revised 29 September 2022  
Accepted 30 September 2022

### KEYWORDS

Calcineurin; mitophagy;  
pancreatic  $\beta$ -cell;  
post-transplantation  
diabetes mellitus; TFEB

## Introduction

Mitochondrial function plays a crucial role in appropriate insulin release from pancreatic  $\beta$ -cells in response to glucose challenge. ATP generation after glucose entry into pancreatic  $\beta$ -cells through citric acid cycle induces closure of  $K^+$ -sensitive ATP channel and subsequent  $Ca^{2+}$  influx due to depolarization of membrane potential, leading to exocytosis of insulin secretory granules [1]. Maintenance of mitochondrial function relies critically on macroautophagy/autophagy of mitochondria or mitophagy that removes damaged or dysfunctional mitochondria, in addition to other processes such as mitochondrial fusion or fission [2]. When mitochondrial damage induces mitochondrial potential loss, PINK1 accumulates on mitochondrial outer membrane, causing activation of ubiquitin and recruitment of PRKN, an E3 ligase for several mitochondrial proteins such as VDAC or MFN


(mitofusin), which is followed by ubiquitination of PRKN substrates, recruitment of autophagy receptors, autophagosome formation and engulfment of dysfunctional mitochondria [3]. Conversely, PRKN-independent mitophagy has also been reported [4].

Autophagy accomplishes degradation of cargo proteins or organelles by their delivery to lysosome via autophagosome fusion with lysosome forming autolysosome. Hence, lysosome is the final effector organelle in the execution of autophagic degradation. Despite the critical role of lysosome in autophagy, relatively little has been known regarding the regulation of lysosomal function or lysosomal steps of autophagic process. However, the recent discovery of *Tfeb* as a master regulator of lysosomal biogenesis and autophagy gene expression has provided a valuable framework to modulate lysosomal function and to construct a model for lysosomal control of autophagic

**CONTACT** Myung-Shik Lee  [mslee0923@sch.ac.kr](mailto:mslee0923@sch.ac.kr)  Soonchunhyang Institute of Medi-bio Science and Division of Endocrinology, Department of Internal Medicine, Soonchunhyang University College of Medicine, Cheonan, 31151, Korea

\*These authors contributed equally to this paper.

This article has been corrected with minor changes. These changes do not impact the academic content of the article.

 Supplemental data for this article can be accessed online at <https://doi.org/10.1080/15548627.2022.2132686>

© 2022 Informa UK Limited, trading as Taylor & Francis Group

activity. Thus, TFEB activation has been reported to be critical in the starvation-induced autophagy and autophagy-mediated lipid catabolism [5,6]. A recent study showed a role of *Tfeb* family members in mitophagy as well [7].

Expression of *Tfeb* is controlled by several transcriptional factors including *Tfeb* itself [5,8,9]. Location and activity of TFEB are controlled post-transcriptionally via phosphorylation of critical residues by kinases such as MTORC1, MAPK1/ERK2 or PRKC/PKC [6,10,11]. TFEB phosphorylation usually leads to binding to YWHA/14-3-3 proteins and inhibition of nuclear translocation, while PRKCB/PKC $\beta$ -mediated TFEB phosphorylation at serine residues near the C-terminal can promote TFEB stabilization and nuclear translocation [12]. On the other hand, phosphatase such as PPP3/calcineurin has been reported to dephosphorylate TFEB at critical residues and to enhance nuclear translocation and activation of TFEB during starvation or stress conditions [13,14]. Regulation of TFEB by PPP3/calcineurin may have clinical implications because PPP3/calcineurin inhibitors that are widely used as immunosuppressive agents have diverse beneficial and adverse clinical effects. One of the major adverse effects of PPP3/calcineurin inhibitors is hyperglycemia that can lead to post-transplantation diabetes mellitus (PTDM). While the pathogenic mechanism of PTDM is still being debated, defective insulin release has been regarded as the main mechanism of diabetes after treatment with PPP3/calcineurin inhibitors [15].

We previously reported that the autophagy of pancreatic  $\beta$ -cells is important not only for pancreatic  $\beta$ -cell mass and structure but also for pancreatic  $\beta$ -cell function [16]. In addition to bulk autophagy, selective autophagy such as mitophagy would also be important in the maintenance of pancreatic  $\beta$ -cell homeostasis and function. Indeed, we recently reported an important role of mitophagy in the functional adaptation of pancreatic  $\beta$ -cells to metabolic stress and also the role of *Tfeb* in this process [14]. Because TFEB can be dephosphorylated and activated by PPP3/calcineurin [13], PPP3/calcineurin inhibitors may be able to inhibit TFEB activation, which may lead to impaired bulk autophagy or selective autophagy such as mitophagy of pancreatic  $\beta$ -cells. We studied whether inhibition of autophagic or mitophagic activity by PPP3/calcineurin inhibitors contributes to the impaired insulin release from pancreatic  $\beta$ -cells, a well-known adverse effect of PPP3/calcineurin inhibitors [17,18], with a focus on the role of *Tfeb* family.

## Results

### Inhibition of mitochondrial stressor-induced mitophagy by PPP3/calcineurin inhibitor

We first studied whether mitophagy induced by the treatment of INS-1 insulinoma cells with mitochondrial stressors [14] is negatively modulated by PPP3/calcineurin inhibitors. When we transfected INS-1 cells with *pMito-Keima*, encoding a pH-dependent fluorescent protein with a mitochondria-targeting sequence [19] and cultured in a neutral environment, Keima fluorescence excited by 440-nm laser light was observed. After treatment with rotenone, a mitochondrial complex I inhibitor

or a combination of oligomycin, an ATP synthase inhibitor, and antimycin A, a mitochondrial complex III inhibitor (O/A) for 18 h, many cells showed punctate fluorescence excited by 590-nm laser light (acidic puncta), indicating lysosomal delivery of mitochondrial Keima and occurrence of mitophagy (Figure 1A), similar to a previous paper [14]. In this condition, pretreatment with 100 ng/ml FK506 that inhibits PPP3/calcineurin activity in complex with FK506-binding protein 12 [20] significantly reduced the number of acidic Mito-Keima puncta representing mitophagy after treatment with rotenone or O/A for 18 h (Figure 1A), indicating that FK506 inhibits mitochondrial stressor-induced mitophagy. When the mitophagy level was assessed by a more objective method for detecting Mito-Keima fluorescence compared to puncta counting, Mito-Keima red:green ratio calculated after confocal microscopy [21] was significantly increased by mitochondrial stressors. Such an increased Mito-Keima red:green ratio was suppressed by FK506 (Figure 1A), supporting data obtained by puncta counting. To confirm these findings using another method of mitophagy detection not using *pMito-Keima*, INS-1 cells were transfected with *mRFP-LC3* and treated with rotenone or O/A for 24 h and then subjected to immunofluorescence using antibody (Ab) to TOMM20 (translocase of the outer mitochondrial membrane 20), a mitochondrial outer membrane protein. In many cells treated with rotenone or O/A, RFP-LC3 puncta that were colocalized with TOMM20 were observed (Figure 1B), which supports the occurrence of mitophagy after treatment with mitochondrial stressors [14]. Here again, pretreatment with 100 ng/ml FK506 significantly reduced the number of RFP-LC3 puncta colocalized with TOMM20 after treatment with rotenone or O/A for 24 h (Figure 1B), indicating inhibition of mitochondrial stressor-induced mitophagy by FK506. To further validate the effect of PPP3/calcineurin inhibition on mitophagy, we employed cyclosporin A (CsA), a classical inhibitor of PPP3/calcineurin [22]. CsA significantly attenuated the increased number of acidic Mito-Keima puncta or Mito-Keima red:green ratio by rotenone or O/A treatment for 18 h (Fig. S1A), indicating that the effect of PPP3/calcineurin inhibitors on mitochondrial stressor-induced mitophagy is not restricted to FK506.

Besides mitochondrial stressor-induced mitophagy, we studied the effect of FK506 on basal mitophagy without mitochondrial stressor treatment that might have housekeeping function [23,24]. Indeed, a small number of mitophagy occurred in *pMito-Keima*-transfected INS-1 cells incubated in a medium for 72 h without rotenone or O/A, and addition of FK506 significantly reduced the number of basal acidic Mito-Keima puncta or Mito-Keima red:green ratio (Figure 1C), suggesting that FK506 can suppress basal mitophagy as well. We additionally studied the effect of FK506 on mitophagy induced by hypoxia that has relevance to pathological conditions [25,26]. Here again, FK506 suppressed mitophagy induced by hypoxia, as detected by acidic Mito-Keima puncta counting or Mito-Keima red:green ratio calculation (Figure 1D).

We also studied whether the effect of FK506 on mitophagy could be due to the possible effect of FK506 on mitochondrial fission because a previous paper reported attenuated

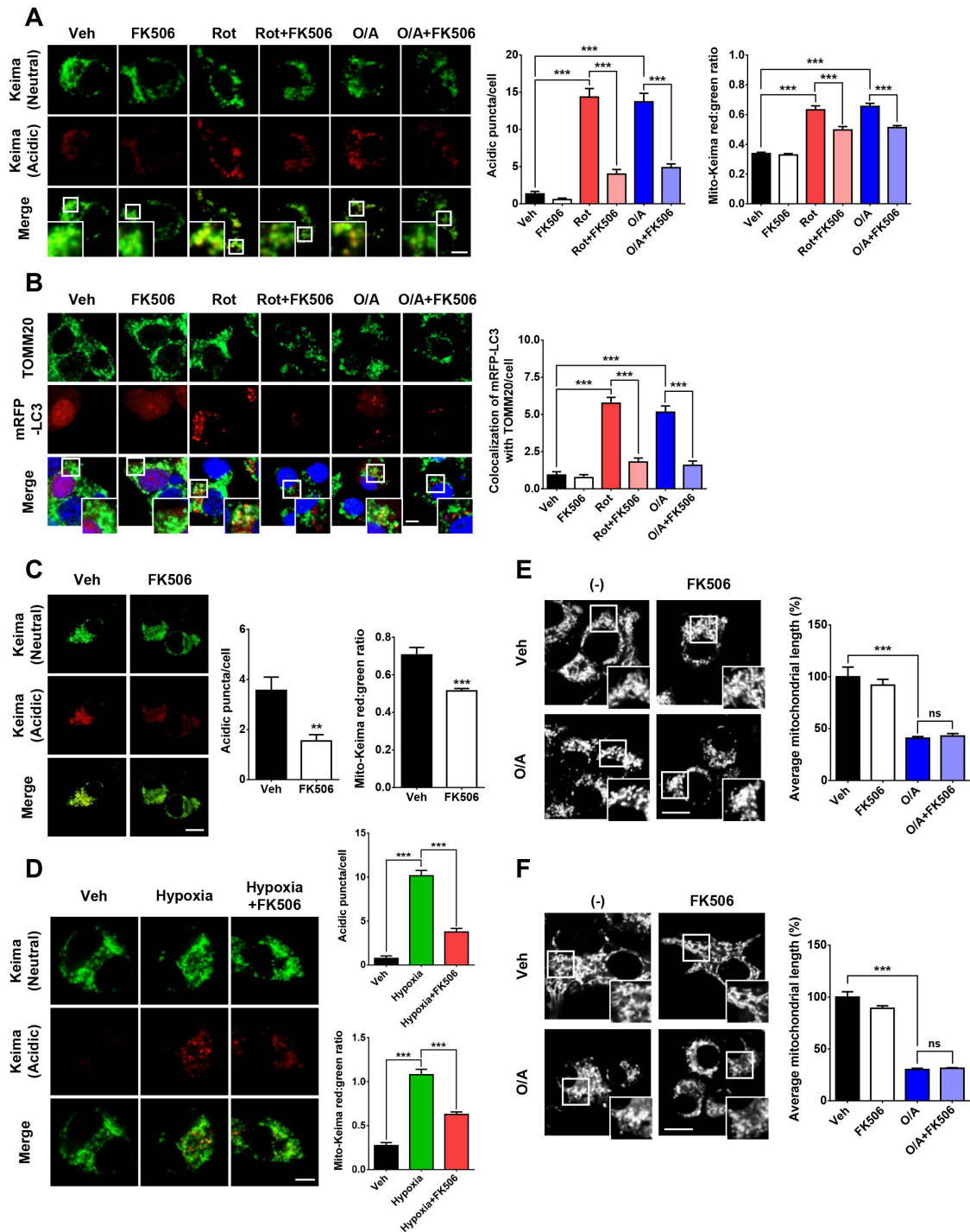


**Figure 1.** Effect of FK506, a PPP3/calcineurin inhibitor, on mitophagy of INS-1 insulinoma cells after treatment with mitochondrial stressors. **(A)** INS-1 cells transfected with *pMito-Keima* plasmid were incubated with rotenone (Rot) or oligomycin+antimycin A (O/A) for 18 h in the presence or absence of FK506 pretreatment. Fluorescent microscopy was performed at excitation wavelengths of 440 and 590 nm to visualize fluorescence from mitochondrial Keima and that from acidic Mito-Keima delivered to lysosome, thus from mitophagy, respectively (left). The number of acidic Mito-Keima puncta per cell (middle) and Mito-Keima red:green ratio representing mitophagy (right) were calculated. Scale bar: 5  $\mu$ m.  $n = 30$  (Veh, vehicle; Rot, rotenone; O/A, oligomycin+antimycin A). **(B)** INS-1 cells transfected with *mRFP-LC3* were treated for 24 h and stained with Ab to TOMM20, a mitochondrial outer membrane protein, to visualize autophagosomes colocalized with TOMM20, thus the occurrence of mitophagy (left). The number of RFP puncta colocalized with TOMM20 was counted (right). Scale bar: 5  $\mu$ m.  $n = 20$ . **(C)** INS-1 cells transfected with *pMito-Keima* were cultured without mitochondrial stressors in the presence or absence of FK506 for 72 h. Fluorescent microscopy was performed as in (A) (left). The number of acidic Mito-Keima puncta per cell (middle) and Mito-Keima red:green ratio representing mitophagy (right) were calculated. Scale bar: 10  $\mu$ m.  $n = 30$ . **(D)** INS-1 cells transfected with *pMito-Keima* were incubated in hypoxic chamber (1%  $O_2$ ) for 24 h with or without FK506. Fluorescence microscopy was performed as in (A) (left). The number of acidic Mito-Keima puncta per cell (right upper) and Mito-Keima red:green ratio representing mitophagy (right lower) were calculated. Scale bar: 5  $\mu$ m.  $n = 20$ . **(E and F)** After O/A treatment of INS-1 cells for 1 (E) or 24 h (F) with or without FK506 pretreatment for 1 h, cells were stained with MitoTracker Green to visualize mitochondria (left). Average length of mitochondria was measured to estimate mitochondrial fission (right). Scale bar: 10  $\mu$ m.  $n = 8$ . Cells in the rectangles were magnified. All data in this figure are the means  $\pm$  SEM from more than three independent experiments.  $^{**}P < 0.01$ ,  $^{***}P < 0.001$  by one-way ANOVA with Tukey's test (**A,B,D,E,F**) or two-tailed *t*-test (**C**). ns: not significant.



mitochondrial fission or fragmentation by PPP3/calcineurin inhibitors that can lead to reduced mitophagy [27]. Treatment of INS-1 cells with O/A for 1 h induced notable mitochondrial fission as revealed by significantly reduced average mitochondrial length (Figure 1E), consistent with a previous paper using other types of cells [28]. Pretreatment with FK506 for 1 h did not significantly affect the mitochondrial length of INS-1 cells treated with O/A (Figure 1E), eliminating the possible contribution of altered mitochondrial fission in FK506-induced inhibition of mitophagy. We also studied mitochondrial fission at the time when mitophagy was determined. Mitochondrial fission was again well observed 24 h after O/A treatment, and FK506 did not affect the average mitochondrial length at this time point (Figure 1F), supporting that FK506-mediated mitophagy inhibition is unrelated to mitochondrial fission.

### Diminished mitochondrial stressor-induced TFEB translocation by PPP3/calcineurin inhibitor

We next investigated the mechanism of mitophagy inhibition by FK506, focusing on the role of TFEB, a member of the MiTF/TFE family, that has been reported to be important in mitochondrial stressor-induced mitophagy [7]. When INS-1 cells transfected with *TFEB* conjugated to *GFP* (*TFEB-GFP*) were treated with rotenone or O/A for 4 h, nuclear translocation of TFEB assessed by calculating nucleus:cytosol fluorescence ratio was apparently observed (Figure 2A), which is consistent with a previous paper and could be due to mitochondrial reactive oxygen species (ROS) inducing lysosomal  $\text{Ca}^{2+}$  release and subsequent activation of PPP3/calcineurin [14]. Similarly, the treatment of INS-1 cells with rotenone or O/A for 4 h induced apparent nuclear translocation of TFE3, another member of MiTF/TFE family, conjugated to *GFP* (*TFE3-GFP*), as assessed by calculating nucleus:cytosol fluorescence ratio (Figure 2B), consistent with a previous paper [14]. In this condition, pretreatment with FK506 significantly reduced nuclear translocation of TFEB-GFP or TFE3-GFP (Figure 2A,B), probably due to the inhibition of PPP3/calcineurin by FK506. To confirm the reduced rotenone- or O/A-induced nuclear translocation of TFEB by FK506, fractionation study was conducted. Indeed, increased nuclear TFEB after treatment with rotenone or O/A was apparently attenuated by the combined treatment with FK506. On the other hand, reduced TFEB content in the cytoplasm of INS-1 cells treated with rotenone or O/A was partly reversed by combined treatment with FK506 (Figure 2C), confirming attenuated rotenone- or O/A-induced nuclear translocation of TFEB by FK506.

We also studied whether attenuation of rotenone- or O/A-induced nuclear translocation can be observed after treatment with another PPP3/calcineurin inhibitors other than FK506. Indeed, CsA significantly suppressed nuclear translocation of TFEB and TFE3 after treatment with rotenone or O/A for 4 h as well (Fig. S1B), supporting that PPP3/calcineurin inhibitors reduce mitochondrial stressor-induced mitophagy through inhibition of nuclear translocation of TFEB or TFE3.

To confirm the role of reduced TFEB activation in FK506-mediated downregulation of mitophagy, we transfected INS-1

cells with a constitutively active human *TFEB* mutant with the deletion of the first 30 N-terminal amino acids (*TFEBNΔ30*) [29]. The expression of *TFEBNΔ30* significantly reversed FK506-mediated suppression of mitophagy (Figure 2D), indicating that inhibition of nuclear translocation of TFEB is responsible for FK506-mediated diminution of mitophagy.

Since FK506 inhibited TFEB activation and subsequent mitophagy, we studied whether the expression of TFEB target genes could be affected by FK506. Expression of mitophagy receptor genes such as *Calcoco2/Ndp52*, *Optn* or *Nbr1* was significantly increased after treatment of INS-1 cells with rotenone or O/A (Fig. S2A), similar to a previous paper [14]. Expression of autophagy genes or lysosomal genes such as *Map1lc3b*, *Clcn7*, *Uvrag*, *Becn1*, *Mcoln1*, *Ctsa*, *Ctsb*, *Ctsd* and *Ctsf* was also increased by rotenone or O/A, again similar to a previous paper [14]. Expression of *Tfeb* and *Tfe3* themselves was increased by rotenone or O/A as well (Fig. S2A). Combined treatment with FK506 significantly suppressed induction of *Clcn7*, *Uvrag*, *Mcoln1*, *Ctsb*, *Ctsd*, *Calcoco2/Ndp52*, *Optn*, *Tfeb* or *Tfe3* expression by rotenone or O/A (Fig. S2A), which could contribute to the suppression of rotenone- or O/A-induced mitophagy by FK506.

We next studied the changes of TFEB phosphorylation by FK506 because FK506 is one of the classical inhibitors of PPP3/calcineurin, a crucial phosphatase for TFEB [20]. When we studied phosphorylation at S142, one of the most important TFEB phosphorylation sites [6], S142 TFEB phosphorylation was markedly attenuated by rotenone or O/A treatment as reported [14] (Fig. S3). Reduced phosphorylation of S142 TFEB by rotenone or O/A was partially reversed by FK506 (Fig. S3), suggesting that FK506 inhibits TFEB activation through diminished dephosphorylation.

We also studied the phosphorylation of S211 of TFEB, a site for 14-3-3 binding that can induce cytoplasmic retention of TFEB [30]. Similar to the phosphorylation of S142 TFEB, that of S211 of TFEB was markedly reduced by rotenone or O/A treatment, which was partially reversed by FK506 (Fig. S3), suggesting that FK506 downregulates TFEB activation through diminished dephosphorylation.

We additionally observed a markedly reduced expression of total TFEB after O/A treatment (Fig. S3), suggesting a possible degradation of TFEB, which is similar to our previous observation [14] and could be due to changes in the phosphorylation of amino acid residues modulating the stability of TFEB family members [12].

### Impairment of mitochondrial function by PPP3/calcineurin inhibitor

We next studied whether impaired mitophagy leads to mitochondrial dysfunction by measuring mitochondrial potential. When INS-1 cells were treated with rotenone for 4 h, a significant proportion of cells with low mitochondrial potential were observed (Fig. S2B). When the medium containing rotenone was replaced with a fresh medium without rotenone for additional culture for 48 h, the proportion of cells with low mitochondrial potential was markedly decreased, suggesting recovery of mitochondrial function (Fig. S2B). When rotenone-containing medium was changed

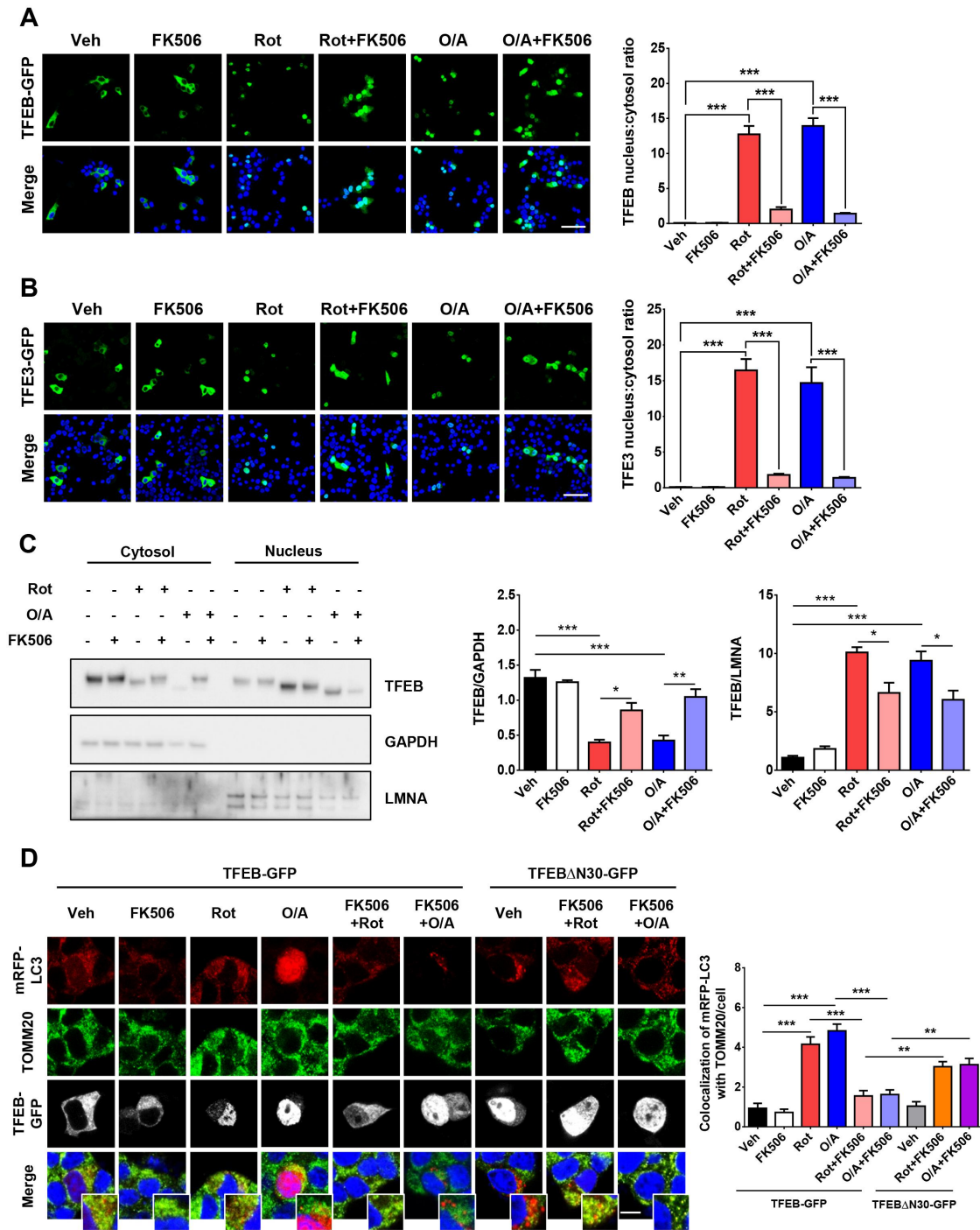


**Figure 2.** Effect of FK506 on TFEB nuclear translocation. **(A)** After treatment of *TFEB-GFP*-transfected INS-1 cells with rotenone or O/A for 4 h with or without FK506 pretreatment for 1 h, fluorescent microscopy was conducted (left). TFEB nucleus:cytosol fluorescence ratio was determined using ImageJ software (right). Scale bar: 50  $\mu$ m. n = 50. **(B)** After rotenone or O/A treatment of *TFE3-GFP*-transfected INS-1 cells with or without FK506 pretreatment as in (A), fluorescent microscopy was conducted (left). TFE3 nucleus:cytosol fluorescence ratio was determined (right). Scale bar: 50  $\mu$ m. n = 50. **(C)** After pretreatment of INS-1 cells with rotenone or O/A with or without pretreatment with FK506, cells were fractionated by centrifugation. Cytoplasmic and nuclear fractions were subjected to immunoblot analysis using the indicated Abs. Densitometric values after ImageJ analysis of the band intensity normalized to that of GAPDH (middle) or LMNA (lamin A) band (right) were compared between groups. Representative immunoblots are presented (left). n = 3. **(D)** After transfection of INS-1 cells with *TFEB-GFP* or constitutively active *TFEBΔN30-GFP* together with *mRFP-LC3*, cells were treated with rotenone or O/A for 4 h with or without FK506 pretreatment for 1 h. After immunostaining with anti-TOMM20 Ab, *mRFP-LC3* puncta colocalized with TOMM20 were visualized by confocal microscopy as in Figure 1B (left). The number of *mRFP-LC3* puncta colocalized with TOMM20 was counted (right). Scale bar: 5  $\mu$ m. n = 20. All data in this figure are the means  $\pm$  SEM from more than three independent experiments. \*P < 0.05, \*\*P < 0.01, \*\*\*P < 0.001 by one-way ANOVA with Tukey's test.

to a fresh medium containing FK506 without rotenone, the proportion of cells with low mitochondrial potential was significantly increased, suggesting that FK506 impairs recovery from mitochondrial injury and mitochondrial dysfunction

probably due to insufficient mitophagy (Fig. S2B). We also studied whether ROS accumulation due to rotenone-induced mitochondrial stress could be affected by FK506. When INS-1 cells were treated with rotenone for 4 h, a significant

accumulation of mitochondrial ROS stained with MitoSOX was observed (Fig. S2C). When the medium containing rotenone was replaced with a fresh medium without rotenone for additional culture for 48 h, mitochondrial ROS accumulation was markedly decreased, suggesting recovery from mitochondrial stress (Fig. S2C). When rotenone-containing medium was changed to a fresh medium containing FK506 without rotenone, reduction of mitochondrial ROS accumulation was significantly less, suggesting that FK506 impairs recovery from mitochondrial stress probably due to insufficient mitophagy (Fig. S2C). We also studied the effect of FK506 on mitophagy during recovery of mitochondrial function. When we determined mitophagy 48 h after the removal of rotenone, mitophagy was lowered to the background level, probably because mitochondrial function was almost completely recovered, and we could not examine the effect of FK506 on mitophagy (data not shown). In contrast, when we determined mitophagy 6 h after the removal of mitochondrial stressors, the number of acidic Mito-Keima puncta was decreased but still detectable probably because mitochondrial function was not completely recovered yet. In this condition, FK506 significantly reduced mitophagy detected by acidic Mito-Keima puncta counting or red:green fluorescence calculation (Fig. S2D), suggesting that FK506-mediated suppression of mitophagy is responsible for impaired recovery of mitochondrial function by FK506.

We additionally determined mitochondrial oxygen consumption rate (OCR) as a measure of mitochondrial function. Basal, ATP-coupled and maximal mitochondrial OCR were significantly reduced by FK506 (Fig. S2E), indicating impaired mitochondrial function by FK506 treatment. Probably due to mitochondrial dysfunction, insulin release in response to glucose challenge was reduced in INS-1 cells treated with FK506 (Fig. S2F).

#### **Amelioration of FK506-induced mitochondrial dysfunction by autophagy enhancer**

We next studied whether enhancement of mitophagy could reverse impaired mitochondrial function of INS-1 cells treated with FK506. To this end, we employed MSL-7 that has been shown to activate TFEB and ameliorate mitochondrial dysfunction associated with metabolic inflammation or human islet amyloid polypeptide oligomer accumulation [31,32]. When INS-1 cells were treated with MSL-7, the number of acidic Mito-Keima puncta per cell was significantly increased both in the presence and absence of FK506, indicating enhanced mitophagy (Figure 3A). Mitophagy level assessed by calculating red:green fluorescence ratio was also significantly enhanced by MSL-7 in the presence or absence of FK506 (Figure 3A). When autophagy enhancers unrelated to PPP3/calcineurin inhibition were employed to avoid possible conflicting effects of FK506 and MSL-7 acting on the same target molecule, spermidine or imatinib [33,34] significantly increased the number of acidic Mito-Keima puncta and red:green fluorescence ratio both in the presence and absence of FK506, demonstrating that diverse autophagy enhancers can override the effect of FK506 on mitophagy (Fig. S4). MSL-7 also increased nuclear translocation of TFEB in untreated

TFEB-GFP-transfected INS-1 cells in the presence and absence of FK506 (Figure 3B), which could be responsible for enhanced mitophagy by MSL-7. To confirm that MSL-7-mediated enhancement of mitophagy in cells treated with FK506 is through TFEB activation, we employed cells with targeted disruption of *Tfeb*. In *Tfeb*-KO INS-1 cells [31], occurrence of mitophagy by MSL-7 or reversal of FK506-mediated suppression of mitophagy by MSL-7 was abrogated as assessed by acidic Mito-Keima puncta counting or calculation of red:green fluorescence ratio (Figure 3C), indicating the role of TFEB activation in MSL-7-mediated enhancement or recovery of mitophagy.

We also studied whether MSL-7 could ameliorate mitochondrial stress imposed by FK506-mediated suppression of mitophagy. When INS-1 cells were pretreated with MSL-7, FK506-mediated increase in cell fraction with low mitochondrial potential after rotenone withdrawal (see Fig. S2B) was significantly attenuated (Figure 4A), suggesting reversal of FK506-mediated suppression of mitochondrial potential recovery by MSL-7. Similarly, FK506-mediated reduction of mitochondrial ROS clearance after rotenone withdrawal (see Fig. S2C) was significantly attenuated by MSL-7 (Figure 4B), suggesting reversal of FK506-mediated inhibition of mitochondrial stress resolution by MSL-7. MSL-7 also significantly reversed FK506-induced suppression of mitophagy observed 6 h after removal of rotenone (Figure 4C). Suppressed basal, ATP-coupled and maximal mitochondrial respirations after FK506 treatment determined by Seahorse respirometry were also significantly restored after combined treatment with MSL-7 (Figure 4D), suggesting that MSL-7 can ameliorate mitochondrial dysfunction induced by PPP3/calcineurin inhibitors. Accordingly, glucose-stimulated insulin release suppressed by FK506 was restored by MSL-7 (Figure 4E). FK506-mediated suppression of rotenone- or O/A-induced *Tfeb*, *Tfe3*, *Uvrag*, *Clcn7*, *Mcoln1*, *Atp6v0e1*, *Calcoco2/Ndp52* and *Optn* expression was also significantly ameliorated by MSL-7 (Figure 4F).

#### **Amelioration of FK506-induced $\beta$ -cell dysfunction by autophagy enhancer**

Since PPP3/calcineurin inhibitors such as FK506 are well-known inducers of PTDM and  $\beta$ -cell dysfunction [35], we studied whether FK506 treatment can cause impairment of insulin release and glucose intolerance in vivo due to inhibition of mitophagy and mitochondrial function. After the administration of 10 mg/kg FK506 daily for 8 weeks, non-fasting blood level was not significantly increased except at eighth week of administration (Figure 5A). Body weight was also not significantly affected by FK506 administration for 8 weeks (Figure 5A). When intraperitoneal glucose tolerance test (GTT) was conducted after administration of 10 mg/kg FK506 for 8 weeks, area under the curve (AUC) was significantly increased indicating glucose intolerance (Figure 5B). Insulinogenic index representing insulin release in response to the changes of glucose concentration and thus  $\beta$ -cell function was also significantly reduced after FK506 treatment for 8 weeks (Figure 5C), suggesting pancreatic  $\beta$ -cell dysfunction after prolonged FK506 treatment in vivo leads to glucose



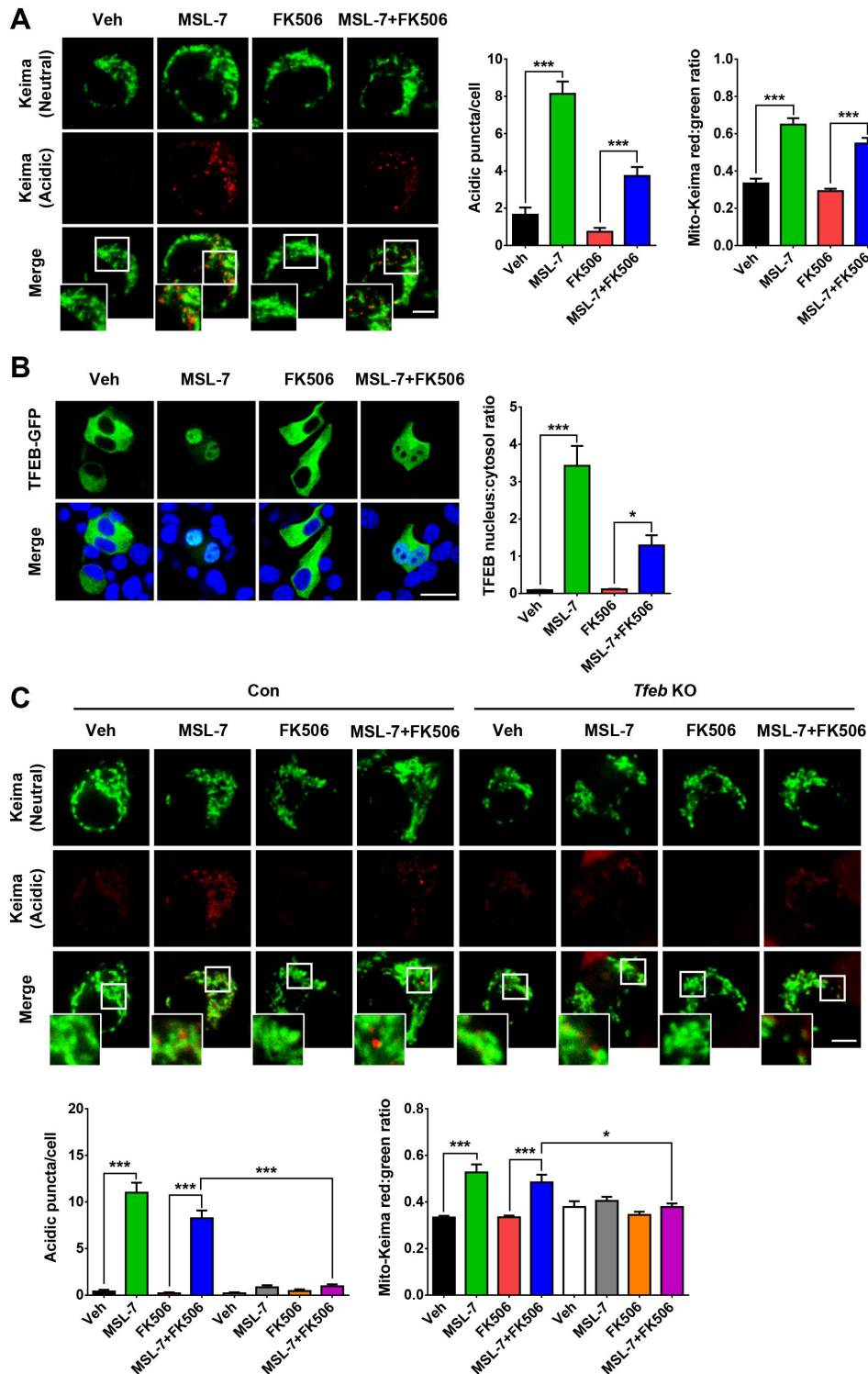


**Figure 3.** Effect of MSL-7, an autophagy enhancer, on FK506-mediated suppression of mitophagy and TFEB nuclear translocation. **(A)** After FK506 treatment of *pMito-Keima*-transfected INS-1 cells for 18 h in the presence or absence of MSL-7 pretreatment for 1 h, fluorescent microscopy was performed as in Figure 1A (left). The number of acidic Mito-Keima puncta (middle) and Mito-Keima red:green ratio representing mitophagy (right) were calculated. Scale bar: 5  $\mu$ m.  $n = 30$ . **(B)** After FK506 treatment for 4 h of *TFEB-GFP*-transfected INS-1 cells with or without MSL-7 pretreatment for 1 h, fluorescent microscopy was conducted (left). TFEB nucleus:cytosol fluorescence ratio was determined (right). Scale bar: 20  $\mu$ m.  $n = 30$ . **(C)** After FK506 treatment of *pMito-Keima*-transfected *Tfeb*-KO INS-1 cells or control cells (Con) for 18 h in the presence or absence of MSL-7 pretreatment for 1 h, fluorescent microscopy was performed to visualize mitophagy as in (A) (upper). The number of acidic Mito-Keima puncta (lower left) and Mito-Keima red:green ratio representing mitophagy (lower right) were calculated. Scale bar: 5  $\mu$ m.  $n = 20$ . Cells in the rectangles were magnified. All data in this figure are the means  $\pm$  SEM from more than three independent experiments. \* $P < 0.05$ , \*\*\* $P < 0.001$  by one-way ANOVA with Tukey's test.

intolerance in these mice. When we studied changes of mitochondrial activity of pancreatic islet cells in mice treated with FK506 for 8 weeks, activity of cytochrome *c* oxidase (COX), mitochondrial complex IV, visualized by diaminobenzidine

tetrahydrochloride (DAB) staining was significantly suppressed (Figure 5D), suggesting mitochondrial dysfunction in pancreatic islet cells could be the cause of pancreatic  $\beta$ -cell dysfunction after FK506 administration.



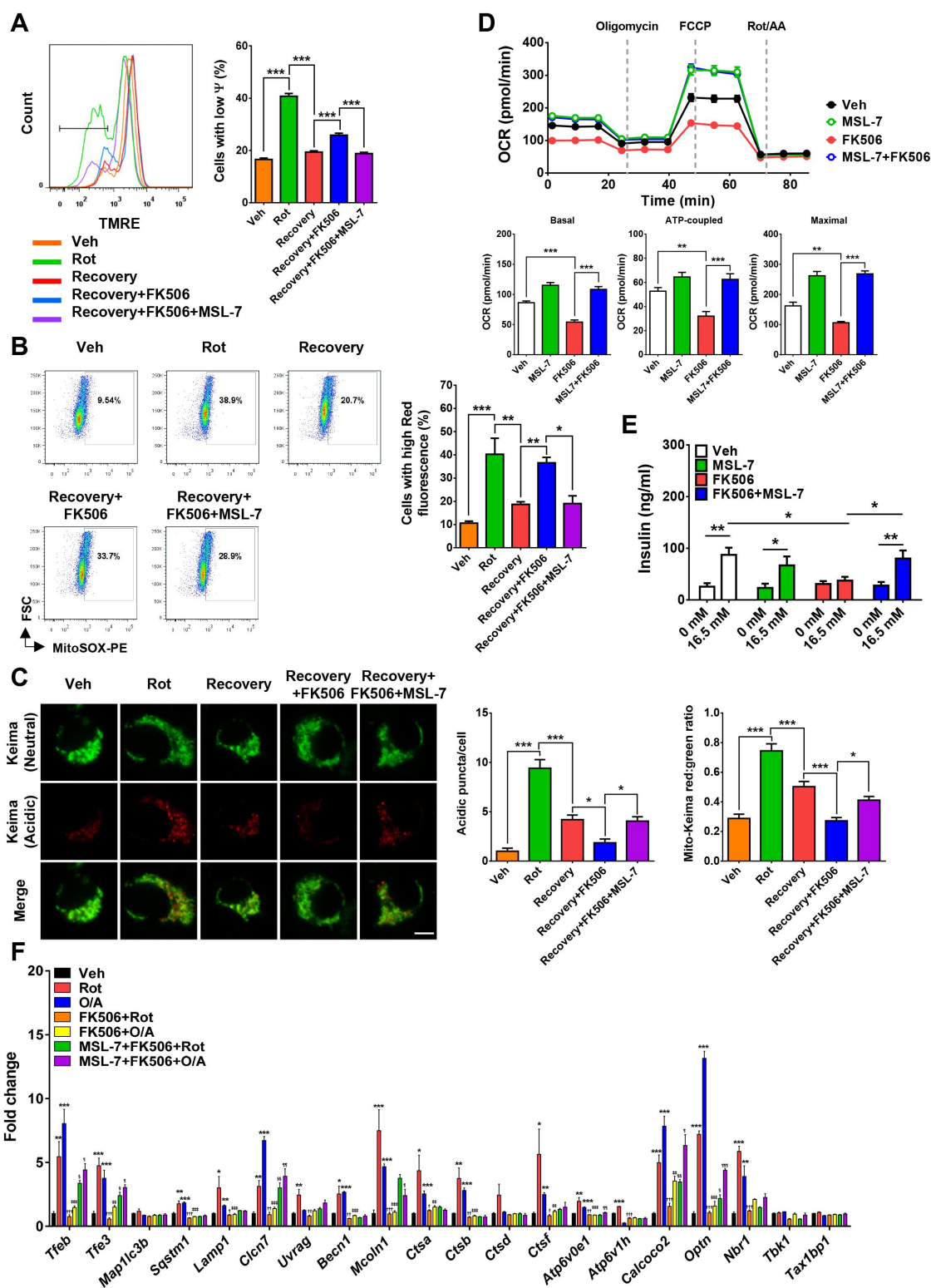


**Figure 4.** Effect of autophagy enhancer on FK506-induced mitochondrial dysfunction. **(A)** Rotenone (Rot)-treated INS-1 cells were allowed to recover in a fresh medium containing FK506 without rotenone in the presence or absence of MSL-7 for 48 h. Mitochondrial potential was determined by flow cytometry after TMRE staining (left). Area representing low mitochondrial potential was calculated (right).  $n = 4$ . **(B)** In INS-1 cells allowed to recover from rotenone-induced mitochondrial stress in a fresh medium containing FK506 without rotenone in the presence or absence of MSL-7 as in (A), mitochondrial ROS was determined using MitoSOX (upper). Representative flow cytometric scattergrams are presented (left).  $n = 4$ . **(C)** INS-1 cells transfected with *pMito-Keima* were incubated with rotenone for 4 h and were allowed to recover in a fresh medium with or without FK506 in the presence or absence of MSL-7 for 6 h. Mito-Keima fluorescence was visualized as in Figure 1A (left). The number of acidic Mito-Keima puncta per cell (middle) and Mito-Keima red:green ratio representing mitophagy (right) were calculated. Scale bar: 5  $\mu$ m.  $n = 20$ . **(D)** Mitochondrial oxygen consumption rate (OCR) was determined in INS-1 cells treated with FK506 for 72 h in the presence or absence of MSL-7 (upper). Basal, ATP-coupled and maximal oxygen consumption were determined from the OCR curves (lower) (AA, antimycin A; FCCP, carbonyl cyanide 4-(trifluoromethoxy)phenylhydrazone).  $n = 6$ . **(E)** Glucose-induced insulin release from INS-1 cells was determined in a medium containing FK506 in the presence or absence of MSL-7 using ELISA, as described in the Material and methods.  $n = 5$ . **(F)** After pretreatment of INS-1 cells with FK506 in the presence or absence of MSL-7, cells were treated with rotenone or O/A for 6 h. Expression of the indicated genes was examined by real-time RT-PCR.  $n = 4$ . All data in this figure are the means  $\pm$  SEM from more than three independent experiments. \*,  $\dagger$ ,  $\S$ ,  $\P < 0.05$ ; \*\*,  $\ddagger$ ,  $\S\S$ ,  $\P\P < 0.01$ ; \*\*\*,  $\dagger\dagger$ ,  $\ddagger\dagger$ ,  $\S\S\S$ ,  $\P\P\P < 0.001$  by one-way ANOVA with Tukey's test. \*, compared to Veh-treated cells;  $\dagger$ , compared to cells treated with Rot alone;  $\ddagger$ , compared to cells treated with O/A alone;  $\S$ , compared to FK506+Rot-treated cells;  $\P$ , compared to FK506+O/A-treated cells.

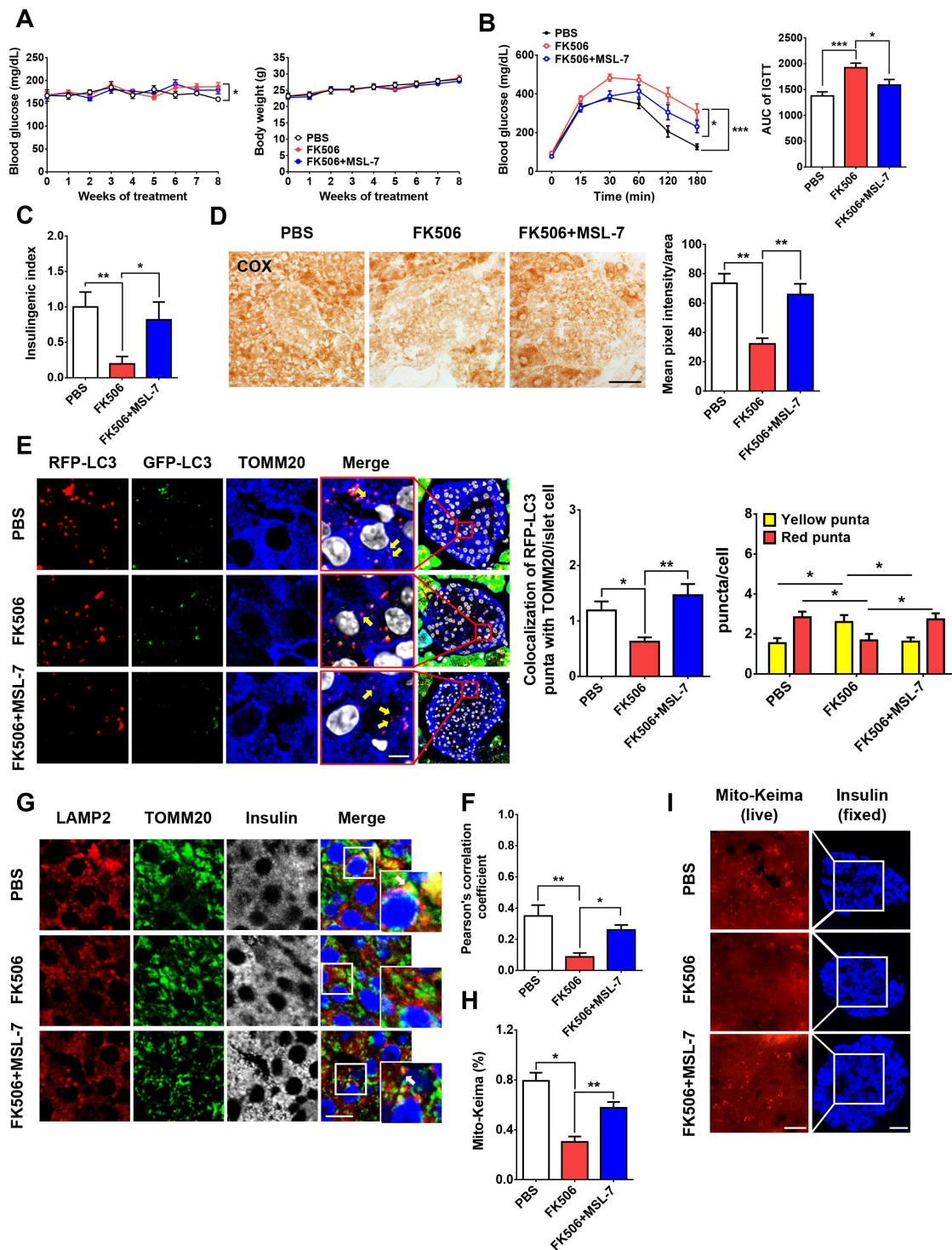


**Figure 5.** Effect of FK506 on glucose profile and  $\beta$ -cell function in vivo. **(A)** C57BL/6 mice were treated with daily administration of 10 mg/kg FK506 for 8 weeks with or without combined administration of 50 mg/kg MSL-7 treatment three times a week. Non-fasting blood glucose (left) and body weight (right) were monitored.  $n = 5$ . **(B)** After treatment of C57BL/6 for 8 weeks as in **(A)**, intraperitoneal GTT was performed (left). Area under the curve (AUC) was calculated (right).  $n = 11$ . **(C)** In mice treated with FK506 as in **(A)**, insulinogenic index was calculated as described in the Materials and methods.  $n = 9-15$ . **(D)** Mitochondrial COX activity in pancreatic islets of mice treated as in **(B)** was determined as described in the Materials and methods, and expressed as the mean pixel intensity per islet area (right). Representative DAB images are presented (left). Scale bar: 50  $\mu$ m.  $n = 5$ . **(E)** *GFP-RFP-LC3*-transgenic mice were treated with daily administration of 10 mg/kg FK506 for 8 weeks with or without combined administration of 50 mg/kg MSL-7 treatment three times a week for 8 weeks. The number of RFP puncta colocalized with TOMM20 in pancreatic islets was counted (middle). Representative fluorescence images of RFP puncta colocalized with TOMM20 are presented (left). The number of red puncta representing autolysosome or autophagic flux and that of yellow puncta representing autophagosome was counted (right). Arrows indicate RFP puncta colocalized with TOMM20. Scale bar: 5  $\mu$ m.  $n = 8-10$ . **(F and G)** In pancreatic sections of the mice of **(E)**, colocalization of LAMP2 spot, a lysosomal marker, with TOMM20 was estimated by Pearson's correlation analysis **(F)**. Representative fluorescence images are presented **(G)**. Arrows indicate LAMP2 spots colocalized with TOMM20. Scale bar: 10  $\mu$ m.  $n = 8$ . **(H and I)** %mitophagy level in pancreatic islets of FK506-injected *Mito-Keima*-transgenic mice with or without combined administration of MSL-7 was calculated as described in the Materials and method **(H)**. Representative Mito-Keima red fluorescence images in pancreatic islets identified by insulin immunofluorescence are presented **(I)**. Scale bar: 10 (boxed areas) or 20  $\mu$ m.  $n = 6-7$ . Cells in the rectangles were magnified. All data in this figure are the means  $\pm$  SEM from more than three independent experiments. \* $P < 0.05$ , \*\* $P < 0.01$ , \*\*\* $P < 0.001$  by one-way ANOVA with Tukey's test **(B-F)** or two-way ANOVA with Bonferroni's test **(A,B)**. ns: not significant.

We next investigated whether the mitophagy of pancreatic islet cells is altered by FK506 treatment in vivo since FK506 reduced mitophagic activity of INS-1 cells in vitro. When we administered FK506 daily for 8 weeks to *CAG-RFP-EGFP-LC3* mice that can be used in vivo assessment of autophagic activity [36], the number of RFP puncta colocalized with TOMM20 was significantly reduced (Figure 5E), indicating reduced mitophagic activity in pancreatic islets of mice treated with FK506 for 8 weeks, which could lead to  $\beta$ -cell dysfunction and diminished insulin release from  $\beta$ -cells. We also employed another method of mitophagy detection in vivo without transgene expression. When we studied the colocalization of TOMM20 with LAMP2, a lysosomal marker protein, as an indicator of mitophagic activity in vivo [37], the number of LAMP2 spots colocalized with TOMM20 was significantly reduced in islets of mice treated with FK506 administration for 8 weeks (Figure 5F,G), suggesting suppressed mitophagy could be the underlying cause of mitochondrial dysfunction, leading to  $\beta$ -cell dysfunction and glucose intolerance after FK506 treatment. To confirm the suppressed mitophagy in pancreatic islets by FK506 treatment using a genetic model dedicated to the assessment of mitophagy in vivo, we employed *Mito-Keima*-transgenic mice [24]. When fresh pancreatic sections were observed under a fluorescent microscope, %mitophagy level was significantly reduced by FK506 treatment for 6 weeks in pancreatic islet area of *Mito-Keima*-transgenic mice identified by insulin immunofluorescence of the adjacent pancreatic section (Figure 5H,I), strongly supporting suppression of mitophagy of pancreatic islets by FK506 administration in vivo.

Using this in vivo model of FK506 administration showing reduced mitophagy or mitochondrial activity in pancreatic islets, glucose intolerance and  $\beta$ -cell dysfunction, we studied whether MSL-7 that could reverse impairment of these parameters by FK506. Administration of 50 mg/kg MSL-7 3 times a week for 8 weeks significantly improved glucose tolerance and insulinogenic index representing  $\beta$ -cell function of mice treated with 10 mg/kg FK506 (Figure 5B,C). Furthermore, MSL-7 administration restored COX activity of pancreatic islets in mice treated with FK506 for 8 weeks (Figure 5D). MSL-7 administration also significantly restored decreased number of RFP-LC3 puncta colocalized with TOMM20 and that of TOMM20 colocalized with LAMP2 after FK506 administration (Figure 5E–G), suggesting that autophagy enhancer MSL-7 can reverse FK506-mediated mitophagy impairment and mitochondrial dysfunction of pancreatic islets, which could be the mechanism of amelioration of FK506-induced glucose intolerance and  $\beta$ -cell dysfunction by autophagy enhancer in vivo. In vivo effect of MSL-7 on the suppression of mitophagy in pancreatic islets by FK506 was also confirmed using *Mito-Keima*-transgenic mice since FK506-mediated suppression of %mitophagy level in pancreatic islets was significantly reversed by MSL-7 treatment in vivo (Figure 5H,I). Since TFEB modulates not only mitophagy but also bulk autophagy, we studied the effect of FK506 and MSL-7 on bulk autophagy by counting the number of total RFP-LC3 puncta in pancreatic islets of FK506-treated mice with or without combined MSL-7 administration. The number of RFP-LC3 puncta representing bulk autophagic flux was significantly diminished in pancreatic islets

by treatment with FK506 for 8 weeks, and combined treatment with MSL-7 reversed the diminished number of RFP-LC3 puncta (Figure 5E). On the other hand, the number of yellow puncta representing autophagosome in pancreatic islets was significantly increased by treatment with FK506 for 8 weeks, and combined treatment with MSL-7 abrogated the increase in the number of yellow puncta (Figure 5E), which suggests that FK506-mediated decrease in bulk autophagic activity was reversed by MSL-7, and that altered bulk autophagy or selective autophagy other than mitophagy might contribute to the FK506-induced  $\beta$ -cell dysfunction and its restoration by MSL-7.

While the most important cause of PTDM induced by PPP3/calcineurin inhibitors is  $\beta$ -cell dysfunction and defective insulin release [15,38], insulin resistance has also been incriminated in PTDM associated with PPP3/calcineurin inhibitors [39]. When we conducted insulin tolerance test (ITT) after 8 weeks of FK506 treatment, a small but significant insulin resistance was observed, which was accompanied by a significantly decreased AUC of ITT curve (Fig. S5A). HOMA-IR index, a measure of insulin resistance [40], was also increased after 8 weeks of FK506 treatment (Fig. S5B), indicating FK506-mediated insulin resistance. Combined administration of MSL-7 did not ameliorate insulin resistance caused by FK506 such as decreased AUC of ITT curve or increased HOMA-IR index (Fig. S5A and B), suggesting that insulin resistance could contribute to FK506-induced glucose intolerance in vivo, which might not be directly related to impaired mitophagy or mitochondrial dysfunction [39].

## Discussion

We observed that FK506, a PPP3/calcineurin inhibitor widely used as an immunosuppressant against graft rejection [20], suppressed mitophagy induced by mitochondrial stressors such as rotenone or O/A and also basal or hypoxia-induced mitophagy that might have housekeeping or pathophysiological role [23–26]. Since antimycin A, a mitochondrial complex III inhibitor, has a relatively weak effect on mitochondrial potential, it has been used in combination with oligomycin to inhibit reverse activity of  $F_1F_0$ -ATPase [41]. Suppression of mitophagy by FK506 was associated with inhibition of TFEB nuclear translocation. CsA, another representative PPP3/calcineurin inhibitor [22], also inhibited TFEB nuclear translocation and mitophagy. Because rotenone or O/A induced robust nuclear translocation of TFEB, most cells with cytosolic TFEB after combined treatment with FK506 due to attenuated rotenone- or O/A-induced TFEB nuclear translocation still displayed remaining nuclear TFEB, rendering counting of cells with suppressed nuclear TFEB translocation ambiguous. However, fractionation study clearly demonstrated suppressed rotenone- or O/A-induced TFEB nuclear translocation by FK506.

Inhibition of TFEB activation by PPP3/calcineurin inhibitors appears to be the most likely cause of suppressed mitophagy because forced expression of a constitutively active mutant of TFEB [29] abrogated FK506-mediated suppression of mitophagy. Inhibition of TFEB nuclear translocation by FK506 was, in turn, due to diminution of



TFEB dephosphorylation by FK506 that inhibits PPP3/calcineurin, one of the most important phosphatases for TFEB [13].

FK506-mediated suppression of mitophagy led to the insufficient recovery of mitochondrial potential or diminished quenching of mitochondrial ROS after removal of mitochondrial stressors, and also reduced mitochondrial oxygen consumption *in vitro*. Furthermore, glucose tolerance, insulinogenic index representing  $\beta$ -cell function, and mitochondrial COX activity or mitophagic activity of islet cells were impaired after *in vivo* treatment with FK506 for 8 weeks. These results suggest that impaired mitochondrial function due to suppressed mitophagy of pancreatic  $\beta$ -cells is an important cause of glucose intolerance,  $\beta$ -cell dysfunction and diabetes after FK506 treatment or PTDM. While these results suggest a crucial role of mitophagy in the maintenance of  $\beta$ -cell function, consistent with a previous paper [14], the role of PRKN, a crucial E3 ligase inducing mitophagy through proteolysis of VDAC or other mitochondrial outer membrane proteins and recruiting autophagy adaptors such as OPTN or CALCOCO2/NDP52 [42,43], in pancreatic  $\beta$ -cell function has been controversial. While the protective role of PRKN in pancreatic  $\beta$ -cell injury has been reported [44], other papers reported no significant reduction of pancreatic  $\beta$ -cell function in mice with  $\beta$ -cell-specific *prkn*-KO or *pink1*-KO mice [45,46]. Such discrepancies could be attributed to adaptive changes associated with *prkn* or *pink1* KO, and a possible contribution of PRKN-independent mitophagy [25,47]. Although significant changes were not observed, subtle changes of glucose tolerance, compromised turnover of mitochondrial proteins and reduced generation of NADH or mitochondrial potential after glucose challenge were observed in  $\beta$ -cell-specific *prkn*-KO mice after prolonged HFD feeding or in *pink1*-KO  $\beta$ -cells [45,46], suggesting that a role of PINK1-PRKN pathway in  $\beta$ -cell mitophagy and homeostasis cannot be totally eliminated, depending on the cellular or environmental context.

Intriguingly, MSL-7, an autophagy enhancer improving TFEB activity through PPP3/calcineurin activation [31,32], was able to reverse adverse effects of FK506 on mitophagy and mitochondrial function *in vitro* and *in vivo*. These results suggest a potential role of MSL-7 in the management of PTDM. PTDM occurring in 10–40% of patients receiving solid organ transplantation is a clinically important risk factor associated with premature cardiovascular diseases and increased mortality in patients with organ transplantation [15]. Immunosuppressants such as PPP3/calcineurin inhibitors, MTOR inhibitors or glucocorticoid are well-known inducers of PTDM. Among PPP3/calcineurin inhibitors, FK506 is associated with a particularly high incidence of PTDM [48]. Molecular mechanisms of PTDM by PPP3/calcineurin inhibitors include the blockade of FK506-binding protein-cyclic ADP ribose interaction, suppression of ATP-sensitive K<sup>+</sup> channel and compromised insulin gene transcription [17,49,50], which finally converge on  $\beta$ -cell dysfunction. Our data suggest that reduced mitophagy leading to mitochondrial dysfunction could be another mechanism accounting for  $\beta$ -cell dysfunction after treatment with PPP3/calcineurin inhibitors.

While  $\beta$ -cell dysfunction is the dominant cause of glucose intolerance and diabetes associated with treatment with PPP3/calcineurin inhibitors [15,38], insulin resistance has also been reported to contribute to the development of diabetes by PPP3/calcineurin inhibitors [39]. In the clinical settings, it would be difficult to delineate the role of PPP3/calcineurin inhibitor itself in the development of insulin resistance and diabetes because other drugs causing insulin resistance such as glucocorticoids are frequently administered together with PPP3/calcineurin inhibitors. Probable mechanisms of insulin resistance by PPP3/calcineurin inhibitors might include reduced SLC2A4/GLUT4-mediated uptake of glucose due to enhanced endocytosis of SLC2A4/GLUT4 and changes of myosin transcription in insulin target tissues [39,51]. Such potential mechanisms of insulin resistance by PPP3/calcineurin inhibitors could be independent of autophagy, mitophagy or mitochondrial function, which can explain the absence of MSL-7 effect on insulin resistance caused by FK506 treatment.

Besides mitophagy, a role of bulk autophagy or other types of selective autophagy cannot be eliminated in FK506-induced  $\beta$ -cell dysfunction and its amelioration by MSL-7, an autophagy enhancer, because FK506 reduced not only mitophagy but also bulk autophagy, and MSL-7 restored diminished bulk autophagy by FK506. Since the role of bulk autophagy in pancreatic  $\beta$ -cell structure, mass and function is well known [16,52], diminished bulk autophagy of  $\beta$ -cells is likely to contribute to the FK506-induced  $\beta$ -cell dysfunction and glucose intolerance, in addition to the reduced mitophagy.

These results suggest that MSL-7, enhancing TFEB activity and autophagic activity, could be a potential therapeutic agent against PTDM. However, rapamycin, another well-known autophagy enhancer inhibiting MTOR, is an inducer of PTDM [15]. Such a discrepancy could be due to the deleterious effects of MTOR inhibitors on  $\beta$ -cell function and insulin sensitivity that could be unrelated to autophagy [53,54]. These results suggest that metabolic outcome of autophagy enhancers *in vivo* might be distinct, depending on the mechanism of autophagy induction.

## Materials and methods

### Cell culture and drugs treatment

INS-1 cells were cultured in RPML-1640 (Welgene, LM 011-01) containing 11.2 mM glucose and 2 mM l-glutamine. The medium was supplemented with 10% FBS, 1 mM pyruvate (Sigma, S8636), 10 mM HEPES, pH 7.4, 50  $\mu$ M 2-mercaptoethanol, 100 U/ml penicillin and 100  $\mu$ g/ml streptomycin. INS-1 cells were seeded onto wells of poly-L-ornithine (Sigma, P4957)-coated plates. For drug treatment, the following concentrations were used: FK506 (100 ng/ml; Invivogen, tlr-fk5), CsA (0.5  $\mu$ g/ml; Invivogen, tlr-cyca), rotenone (100 nM; Sigma, R8875), oligomycin (200 nM; Millipore, 495455), antimycin A (125 nM; Sigma, A8674), MSL-7 (10  $\mu$ M), spermidine (100  $\mu$ M; Sigma, S2626) and imatinib (10  $\mu$ M; Sigma, SML1027). MSL-7 was dissolved in dimethyl sulfoxide (DMSO) to make 10 mM and directly diluted to the final concentrations in culture medium for *in vitro* experiments.



### Transfection and plasmids

Cells were transiently transfected with plasmids such as *pMito-Keima*, *TFEB-GFP*, *TFE3-GFP*, *mRFP-LC3* or *TFEBNΔ30* [29], using lipofectamine 2000 (Invitrogen, 11668019) according to the manufacturer's protocol.

### Cell fractionation

INS-1 cells were treated with rotenone or O/A for 4 h with or without FK506 pretreatment for 1 h. After washing cells with PBS (Welgene, LB 001-01), fractionation was performed using Nuclear/Cytosol Fractionation Kit (BioVision, K266), according to the manufacturer's protocol.

### Immunoblot analysis

Cells were solubilized in a lysis buffer containing protease inhibitors (Sigma, 11697498001). Protein concentration was determined using the Bradford method. Samples (10~30 μg) were loaded onto 4 12% Bis-Tris gel (Bolt; Invitrogen, NW04125BOX), and transferred to nitrocellulose membranes for immunoblot analysis using the enhanced chemiluminescence method (Dongin LS, ECL-PS250). Abs against the following proteins were used: TFEB (Bethyl Laboratories, A303-673A; 1:1,000), phospho-S142-TFEB (Millipore, ABE1971; 1:1,000), phospho-S211-TFEB (Cell Signaling Technology, 37681S; 1:1,000), ACTB (Santa Cruz Biotechnology, sc-47,778; 1:1,000), GAPDH (Santa Cruz Biotechnology, sc-32,233; 1:1,000) and LMNA/lamin A (Santa Cruz Biotechnology, sc-71,481; 1:1,000). Densitometry of the protein bands was determined using ImageJ software.

### Detection of mitophagy in vitro

To visualize mitophagy using a mitophagy-specific probe, INS-1 cells were transfected with *pMito-Keima* (MBL, AM-V0251), and then treated with rotenone or O/A for 18 h in the presence or absence of FK506 or CsA. To examine basal mitophagy, cells were treated with FK506 for 72 h. To determine hypoxia-induced mitophagy, INS-1 cells were incubated in a hypoxic chamber (1% O<sub>2</sub>) for 24 h with or without FK506. Keima fluorescence at neutral pH was observed at an excitation wavelength of 430 ± 20 nm and an emission wavelength of 624 ± 20 nm. Keima fluorescence in acidic conditions was observed at an excitation wavelength of 562 ± 20 nm and an emission wavelength of 624 ± 20 nm. Acidic Mito-Keima puncta or fluorescence ratio was quantified using ImageJ or ZEN software. To visualize mitophagy in another way, cells transfected with the *mRFP-LC3* construct were treated with mitochondrial stressors and then incubated with anti-TOMM20 Ab (Cell Signaling Technology, 42406S; 1:200). Images were obtained using an LSM780 confocal microscope (Zeiss), and the colocalization between RFP puncta and TOMM20 staining was counted as a marker of mitophagy [55]. Colocalization of puncta was evaluated manually in a blinded manner.

### Insulin secretion

INS-1 cells were treated with FK506 for 72 h and pre-incubated at 37°C for 30 min in Krebs–Ringer bicarbonate (KRB) buffer containing 115 mM NaCl, 5 mM KCl, 1 mM MgCl<sub>2</sub>, 2.5 mM CaCl<sub>2</sub>, 25 mM NaHCO<sub>3</sub>, 25 mM HEPES, pH 7.4, supplemented with 0.5% bovine serum albumin (GenDEPOT, A0100-010). The pre-incubation medium was then replaced with KRB buffer supplemented with different concentrations of glucose (basal: 0 mM; stimulatory: 16.5 mM). After incubation for 1 h at 37°C, the supernatant was collected and stored at –80°C for determination of insulin content Mouse insulin ELISA KIT (TMB; Shibayagi, AKRIN-011T).

### Mitochondrial membrane potential and ROS

To determine mitochondrial potential and ROS, INS-1 cells were treated with rotenone for 4 h. After washout of rotenone, additional culture was conducted in a medium containing FK506 with or without MSL-7 for 48 h. INS-1 cells were then stained with 300 nM tetramethylrhodamine ethyl ester (TMRE, Invitrogen, T669) and 5 μM MitoSOX (Invitrogen, M36008), respectively, at 37°C for 30 min. Cells were suspended in PBS-1% FBS for analysis on a FACSVerse (BD Biosciences) using FlowJo software (TreeStar).

### Mitochondrial length

INS-1 cells were treated with O/A for 1 h or 24 h with or without FK506 pretreatment for 1 h, and then stained with 200 nM MitoTracker Green (Invitrogen, M7514) at 37°C for 30 min. Images were obtained using an LSM780 confocal microscope (Zeiss). Quantification of the average of mitochondrial length was performed using ImageJ software.

### RNA extraction and real-time RT-PCR

cDNA was synthesized using total RNA extracted with TRIzol (Invitrogen, 15596018) and *M-MLV* Reverse Transcriptase (Promega, M1701), according to the manufacturer's instruction. Real-time RT-PCR was conducted using SYBR green (Takara, RR420A) in a QuantStudio3 Real-Time PCR System (Applied Biosystems). Expression values were normalized to the *Rpl32* mRNA level. Sequences of primers used for real-time RT-PCR are listed in Table S1.

### Animals

Eight-week-old C57BL/6N or *CAG-RFP-EGFP-LC3*-transgenic mice (Jackson Laboratory, 027139) were maintained in a 12-h light/12-h dark cycle and fed a chow diet. Ten mg/kg FK506 or vehicle was administered intraperitoneally daily for 8 weeks. FK506 was dissolved in DMSO to make a 100 mg/ml stock solution, which was diluted with PBS to 1 mg/ml before injection. In an experiment to study the effect of autophagy enhancer in vivo, MSL-7 (50 mg/kg) or vehicle was administered intraperitoneally three times a week together with 10 mg/kg FK506 intraperitoneal administration daily for 8 weeks. MSL-7 was dissolved in DMSO to yield a 50

mg/ml stock solution, which was diluted with PBS to 5 mg/ml before injection. During the observation period, mice were monitored for glucose profile and weighed. *Mito-Keima*-transgenic mice [24] backcrossed more than seven times to C57BL/6J mice were maintained in a 12-h light/12-h dark cycle and fed a chow diet. Eight 12-week-old *Mito-Keima*-transgenic mice were injected with 10 mg/kg FK506 daily with or without 50 mg/kg MSL-7 administration three times a week for 6 weeks. All animal experiments were conducted in the vivarium of Yonsei University College of Medicine or Ewha Womans University, in accordance with the Public Health Service Policy in the Humane Care and Use of Laboratory Animals. Mouse experiments were approved by the IACUC of Yonsei University College of Medicine or Ewha Womans University.

### Detection of mitophagy in vivo

Tissue sections from *CAG-RFP-EGFP-LC3*-transgenic mice prepared as described [56] were subjected to fluorescent microscopy after immunostaining using anti-TOMM20 Ab and DAPI staining to identify RFP puncta colocalized with TOMM20, thus the occurrence of mitophagy. To evaluate mitophagy in vivo without transgene, after immunohistochemistry of paraffin-embedded pancreatic sections of C57BL/6 mice treated with FK506 alone or FK506 and MSL-7 using anti-LAMP2 (Abcam, ab13524; 1:200), -TOMM20 and -insulin (Cell Signaling Technology, 4590S; 1:200) Abs, colocalization between LAMP2 and TOMM20 was assessed by calculating Pearson's correlation coefficient [37].

Mitophagy levels in *Mito-Keima*-transgenic mice were assessed by confocal microscopy essentially as described previously [24,57]. To analyze *Mito-Keima* fluorescence signal in pancreatic islets of *Mito-Keima*-transgenic mice, one of the two consecutive fresh pancreatic cryosections of 8  $\mu$ m thickness was fixed in 4% formaldehyde in PBS and then subjected to insulin immunofluorescence according to a previously reported method using anti-insulin Ab (Cell Signaling Technology, 4590S; 1:100) [14]. The adjacent section was subjected to confocal microscopy (LSM 800, Zeiss) to visualize *Mito-Keima* fluorescence. *Mito-Keima* fluorescence image was obtained using two sequential excitation lasers (488 and 555 nm) and a 595–700 nm emission bandwidth. Quantitation of mitophagy was conducted using ZEN software, as described [24,57]. %mitophagy level was defined as the number of pixels with a red:green ratio of >1.5 divided by the total number of pixels. More than five tissue samples were studied to calculate the average values of the mitophagy level.

### Intraperitoneal GTT, insulinogenic index and insulin tolerance tests (ITT)

GTT was performed by intraperitoneal injection of 2 g/kg glucose after overnight fasting. Blood glucose concentrations were determined using a One Touch glucometer (Lifescan) before (0 min) and 15, 30, 60, 120 and 180 min after glucose injection. Insulinogenic index was calculated as follows:  $\Delta$ insulin<sub>15 min</sub> (pM)/ $\Delta$ glucose<sub>15 min</sub> (mM), as described [58]. ITT was conducted by injecting intraperitoneally 1 U/kg of

regular insulin to fasted mice and measuring blood glucose levels at 0, 15, 30, 60 and 120 min. Serum insulin was measured using the Mouse insulin ELISA kit. HOMA-IR was calculated using the following formula: (fasting insulin  $\times$  fasting glucose)/22.5.

### COX staining

In vivo detection of COX activity was conducted as described [59]. Briefly, unfixed cryosections of the pancreas were incubated in a reaction buffer containing 10 mg CYCS/cytochrome *c* (Sigma, C2436), 5 mg DAB (Sigma, D5637), 9 ml sodium phosphate buffer (0.1 M, pH 7.4) and 1 ml of 20  $\mu$ g/ml CAT/catalase solution (Sigma, C9322). COX activity was visualized with a standard DAB reaction. Images were acquired with a light microscope and analyzed using ImageJ software.

### Bioenergetic analysis of OCR

Oxygen consumption of INS-1 cells was measured using a Seahorse Extracellular Flux Analyzer (XF24 or XFe96) (Agilent Technologies) equipped with a spheroid microplate-compatible thermal tray according to a modification of the manufacturer's protocol. Briefly, INS-1 cells were plated at 200,000 cells/well onto poly-L-ornithine-coated XF24 microplate or at 5,000 cells/well onto poly-L-ornithine-coated XF96 microplate, and then treated with 100 ng/ml FK506 for 72 h in the presence or absence of MSL-7. After incubation of INS-1 cells with pre-warmed XF assay medium (Seahorse XF base DMEM supplemented with 11 mM glucose, 1 mM sodium pyruvate and 2 mM glutamine) at 37°C for 1 h in a non-CO<sub>2</sub> incubator, cells were sequentially exposed to 1  $\mu$ M oligomycin, 0.5  $\mu$ M FCCP and 0.5  $\mu$ M rotenone+antimycin A at the indicated time points to measure basal, ATP-coupled, maximal and non-mitochondrial oxygen consumption, respectively. Oxygen consumption was analyzed using a WaveTM software (Agilent Technologies).

### Statistical analysis

All values are expressed as the means  $\pm$  SEM of  $\geq 3$  independent experiments performed in triplicate. Two-tailed Student's *t*-test was used to compare values between the two groups. One-way ANOVA with Tukey's test was used to compare values between multiple groups. Two-way repeated-measures ANOVA with Bonferroni's post-hoc test was employed to compare multiple repeated measurements between groups. *P* values <0.05 were considered to represent statistically significant differences.

### Acknowledgments

We thank Jae-Ho Cheong for Seahorse respirometry. *mRFP-LC3* was gifted from Yoshimori T. INS-1 cells were from Wollheim C.

### Disclosure statement

M.-S. L. is the CEO of LysoTech, Inc.

## Funding

This study was supported by a National Research Foundation of Korea (NRF) grant funded by the Korean government (MSIT) (NRF-2019R1A2C3002924) and by the Bio&Medical Technology Development Program (2017M3A9G7073521). M-S Lee is the recipient of a grant from A3 Foresight Program of the NRF (2015K2A2A6002060) and the Participation Grant on the International Academic Association (2022) of the National Academy of Sciences, Korea.

## ORCID

Kihyouon Park  <http://orcid.org/0000-0002-3010-4746>  
 Seong Keun Sonn  <http://orcid.org/0000-0001-8292-3199>  
 Seungwoon Seo  <http://orcid.org/0000-0003-1206-2412>  
 Jinyoung Kim  <http://orcid.org/0000-0002-3810-8549>  
 Goo Taeg Oh  <http://orcid.org/0000-0002-1104-1698>  
 Myung-Shik Lee  <http://orcid.org/0000-0003-3292-1720>

## References

- Nichols CG, Shyng SL, Nestorowicz A, et al. Adenosine diphosphate as an intracellular regulator of insulin secretion. *Science*. 1996;272(5269):1785–1787. DOI:10.1126/science.272.5269.1785
- Mizushima N, Komatsu M. Autophagy: renovation of cells and tissues. *Cell*. 2011;147(4):728–741.
- Narendra D, Tanaka A, Suen DF, et al. Parkin is recruited selectively to impaired mitochondria and promotes their autophagy. *J Cell Biol*. 2008;183(5):795–803. DOI:10.1083/jcb.200809125
- Wei H, Liu L, Chen Q. Selective removal of mitochondria via mitophagy: distinct pathways for different mitochondrial stress. *Biochim Biophys Acta*. 2015;1853(10):2784–2790.
- Settembre C, De Cegli R, Mansueto G, et al. TFEB controls cellular lipid metabolism through a starvation-induced autoregulatory loop. *Nat Cell Biol*. 2013;15(6):647–658. DOI:10.1038/ncb2718
- Settembre C, Di Malta C, Polito VA, et al. TFEB links autophagy to lysosomal biogenesis. *Science*. 2011;332(6036):1429–1433. DOI:10.1126/science.1204592
- Nezich CL, Wang C, Fogel A, et al. MiT/TFE transcription factors are activated during mitophagy downstream of Parkin and Atg5. *J Cell Biol*. 2015;210(3):435–450. DOI:10.1083/jcb.201501002
- Lee JM, Wagner M, Xiao R, et al. Nutrient-sensing nuclear receptors coordinate autophagy. *Nature*. 2014;516(7529):112–115. DOI:10.1038/nature13961
- Seok S, Fu T, Choi SE, et al. Transcriptional regulation of autophagy by an FXR–CREB axis. *Nature*. 2014;516(7529):108–111. DOI:10.1038/nature13949
- Li Y, Xu M, Ding X, et al. Protein kinase C controls lysosome biogenesis independently of mTORC1. *Nat Cell Biol*. 2016;18(10):1065–1077. DOI:10.1038/ncb3407
- Settembre C, Zoncu R, Medina DL, et al. A lysosome-to-nucleus signalling mechanism senses and regulates the lysosome via mTOR and TFEB. *Embo J*. 2012;31(5):1095–1108. DOI:10.1038/emboj.2012.32
- Ferron M, Settembre C, Shimazu J, et al. A RANKL–PKC $\beta$ –TFEB signaling cascade is necessary for lysosomal biogenesis in osteoclasts. 2013;27(8):955–969. DOI:10.1101/gad.213827.113
- Medina DL, Di Paola S, Peluso I, et al. Lysosomal calcium signalling regulates autophagy through calcineurin and TFEB. *Nat Cell Biol*. 2015;17(3):288–299. DOI:10.1038/ncb3114
- Park K, Lim H, Kim J, et al. Lysosomal Ca<sup>2+</sup>-mediated TFEB activation modulates mitophagy and functional adaptation of pancreatic  $\beta$ -cells to metabolic stress. *Nat Commun*. 2022;13(1):1300. DOI:10.1038/s41467-022-28874-9
- Jenssen T, Hartmann A. Post-transplant diabetes mellitus in patients with solid organ transplants. *Nat Rev Endocrinol*. 2019;15(3):172–188.
- Jung HS, Chung KW, Kim JW, et al. Loss of autophagy diminishes pancreatic  $\beta$  cell mass and function with resultant hyperglycemia. *Cell Metab*. 2008;8(4):318–324. DOI:10.1016/j.cmet.2008.08.013
- Okamoto H, Takasawa S. Recent advances in the Okamoto model: the CD38-cyclic ADP-ribose signal system and the regenerating gene protein (Reg)-Reg receptor system in beta-cells. *Diabetes*. 2002;51(S3):462–473.
- Tze WJ, Tai J, Cheung S. In vitro effects of FK-506 on human and islet cells. *Transplantation*. 1990;49(6):1172–1174.
- Katayama H, Kogure T, Mizushima N, et al. A sensitive and quantitative technique for detecting autophagic events based on lysosomal delivery. *Chem Biol*. 2011;18(8):1042–1052. DOI:10.1016/j.chembiol.2011.05.013
- Dumont FJ. FK506, an immunosuppressant targeting calcineurin function. *Curr Med Chem*. 2000;7(7):731–748.
- Luciani A, Schumann A, Berquez M, et al. Impaired mitophagy links mitochondrial disease to epithelial stress in methylmalonyl-CoA mutase deficiency. *Nat Commun*. 2020;11(1):970. DOI:10.1038/s41467-020-14729-8
- Matsuda S, Koyasu S. Mechanisms of action of cyclosporine. *Immunopharmacology*. 2000;47(2–3):119–125.
- Montava-Garriga L, Ganley IG. Outstanding questions in mitophagy: what we do and do not know. *J Mol Biol*. 2020;432(1):206–230.
- Sun N, Yun J, Liu J, et al. Measuring in vivo mitophagy. *Mol Cell*. 2015;60(4):685–696. DOI:10.1016/j.molcel.2015.10.009
- Liu L, Feng D, Chen G, et al. Mitochondrial outer-membrane protein FUNDC1 mediates hypoxia-induced mitophagy in mammalian cells. *Nat Cell Biol*. 2012;14(2):177–185. DOI:10.1038/ncb2422
- Wu H, Chen Q. Hypoxia activation of mitophagy and its role in disease pathogenesis. *Antioxid Redox Signal*. 2015;22(12):1032–1046.
- Cereghetti GM, Costa V, Scorrano L. Inhibition of Drp1-dependent mitochondrial fragmentation and apoptosis by a polypeptide antagonist of calcineurin. *Cell Death Differ*. 2010;17(11):1785–1794.
- De Vos KJ, Allan VJ, Grierson AJ, et al. Mitochondrial function and actin regulate dynamin-related protein 1-dependent mitochondrial fission. *Curr Biol*. 2005;15(7):678–683. DOI:10.1016/j.cub.2005.02.064
- Kim J, Kim SH, Kang H, et al. TFEB–GDF15 axis protects against obesity and insulin resistance as a lysosomal stress response. *Nat Metab*. 2021;3(3):410–427. DOI:10.1038/s42255-021-00368-w
- Roczniak-Ferguson A, Petit CS, Froehlich F, et al. The transcription factor TFEB links mTORC1 signaling to transcriptional control of lysosome homeostasis. *Sci Signal*. 2012;5(228):ra42. DOI:10.1126/scisignal.2002790
- Kim J, Park K, Kim MJ, et al. An autophagy enhancer ameliorates diabetes of human IAPP-transgenic mice through clearance of amyloidogenic oligomer. *Nat Commun*. 2021;12(1):183. DOI:10.1038/s41467-020-20454-z
- Lim H, Lim Y-M, Kim KH, et al. A novel autophagy enhancer as a therapeutic agent against metabolic syndrome and diabetes. *Nat Commun*. 2018;9(1):1438. DOI:10.1038/s41467-018-03939-w
- Eisenberg T, Knauer H, Schauer A, et al. Induction of autophagy by spermidine promotes longevity. *Nat Cell Biol*. 2009;11(11):1305–1314. DOI:10.1038/ncb1975
- Lim Y-M, Lim H-J, Hur KY, et al. Systemic autophagy insufficiency compromises adaptation to metabolic stress and facilitates progression from obesity to diabetes. *Nat Commun*. 2014;5(1):4934. DOI:10.1038/ncomms5934
- Dai C, JT W, Shostak A, et al. Tacrolimus- and sirolimus-induced human  $\beta$  cell dysfunction is reversible and preventable. *JCI Insight*. 2020;5(1):e130770. DOI:10.1172/jci.insight.130770
- Li L, Wang ZV, Hill JA, et al. New autophagy reporter mice reveal dynamics of proximal tubular autophagy. *J Am Soc Nephrol*. 2014;25(2):305–315. DOI:10.1681/ASN.2013040374

- [37] Fang EF, Hou Y, Palikaras K, et al. Mitophagy inhibits amyloid- $\beta$  and tau pathology and reverses cognitive deficits in models of Alzheimer's disease. *Nature Neurosci.* 2019;22(3):401–412. DOI:10.1038/s41593-018-0332-9
- [38] David-Neto E, Lemos FC, Fadel LM, et al. The dynamics of glucose metabolism under calcineurin inhibitors in the first year after renal transplantation in nonobese patients. *Transplantation.* 2007;85(1):50–55. DOI:10.1097/01.tp.0000267647.03550.22
- [39] Chakkeri HA, Kudva Y, Kaplan B. Calcineurin inhibitors: pharmacologic mechanisms impacting both insulin resistance and insulin secretion leading to glucose dysregulation and diabetes mellitus. *Clin Pharmacol Ther.* 2017;101(1):114–120.
- [40] Radziuk J. Insulin sensitivity and its measurement: structural commonalities among the methods. *J Clin Endocrinol Metab.* 2000;85(12):4426–4433.
- [41] Georgakopoulos ND, Wells G, Campanella M. The pharmacological regulation of cellular mitophagy. *Nat Chem Biol.* 2017;13(2):136–146.
- [42] Heo J-M, Ordureau A, Paulo JA, et al. The PINK1-PARKIN mitochondrial ubiquitylation pathway drives a program of OPTN/NDP52 recruitment and TBK1 activation to promote mitophagy. *Mol Cell.* 2015;60(1):7–20. DOI:10.1016/j.molcel.2015.08.016
- [43] Narendra DP, Youle RJ. Targeting mitochondrial dysfunction: role for PINK1 and Parkin in mitochondrial quality control. *Antioxid Redox Signal.* 2011;14(10):1929–1939.
- [44] Hoshino A, Ariyoshi M, Okawa Y, et al. Inhibition of p53 preserves Parkin-mediated mitophagy and pancreatic  $\beta$ -cell function in diabetes. *Proc Natl Acad Sci, USA.* 2014;111(8):3116–3121. DOI:10.1073/pnas.1318951111
- [45] Corsa CAS, Pearson GL, Renberg A, et al. The E3 ubiquitin ligase Parkin is dispensable for metabolic homeostasis in murine pancreatic  $\beta$  cells and adipocytes. *J Biol Chem.* 2019;294(18):7296–7307. DOI:10.1074/jbc.RA118.006763
- [46] Deas E, Piipari K, Machhada A, et al. PINK1 deficiency in  $\beta$ -cells increases basal insulin secretion and improves glucose tolerance in mice. *Open Biol.* 2014;4(5):144051. DOI:10.1098/rsob.140051
- [47] Guerroué F L, Eck F, Jung J, et al. Autophagosomal content profiling reveals an LC3C-dependent piecemeal mitophagy pathway. *Mol Cell.* 2017;68(4):786–796. DOI:10.1016/j.molcel.2017.10.029
- [48] Vincenti F, Friman S, Scheuermann E, et al. Results of an international, randomized trial comparing glucose metabolism disorders and outcome with cyclosporine versus tacrolimus. *Am J Transplant.* 2007;7(6):1506–1514. DOI:10.1111/j.1600-6143.2007.01749.x
- [49] Fuhrer DK, Kobayashi M, Jiang H. Insulin release and suppression by tacrolimus, rapamycin and cyclosporin a are through regulation of the ATP-sensitive potassium channel. *Diabetes Obes Metab.* 2001;3(6):393–402.
- [50] Hernández-Fisac I, Pizarro-Delgado J, Calle C, et al. Tacrolimus-induced diabetes in rats courses with suppressed insulin gene expression in pancreatic islets. *Am J Transplant.* 2007;7(11):2455–2462. DOI:10.1111/j.1600-6143.2007.01946.x
- [51] Pereira MJ, Palming J, Rizell M, et al. Cyclosporine a and tacrolimus reduce the amount of GLUT4 at the cell surface in human adipocytes: increased endocytosis as a potential mechanism for the diabetogenic effects of immunosuppressive agents. *J Clin Endocrinol Metab.* 2014;99(10):E1885–1894. DOI:10.1210/jc.2014-1266
- [52] Ebato C, Uchida T, Arakawa M, et al. Autophagy is important in islet homeostasis and compensatory increase of beta cell mass in response to high-fat diet. *Cell Metab.* 2008;8(4):325–332. DOI:10.1016/j.cmet.2008.08.009
- [53] Barlow AD, Nicholson ML, Herbert TP. Evidence for rapamycin toxicity in pancreatic  $\beta$ -cells and a review of the underlying molecular mechanisms. *Diabetes.* 2013;62(8):2674–2682.
- [54] Sarbessov DD, Ali SM, Sengupta S, et al. Prolonged rapamycin treatment inhibits mTORC2 assembly and Akt/PKB. *Mol Cell.* 2006;22(2):159–168. DOI:10.1016/j.molcel.2006.03.029
- [55] Zou J, Yue F, Li W, et al. Autophagy inhibitor LRPPRC suppresses mitophagy through interaction with mitophagy initiator Parkin. *PLoS One.* 2014;9:e94903.
- [56] Mizushima N, Yamamoto A, Matsui M, et al. In vivo analysis of autophagy in response to nutrient starvation using transgenic mice expressing a fluorescent autophagosome marker. *Mol Biol Cell.* 2004;15(3):1101–1111. DOI:10.1091/mbc.e03-09-0704
- [57] Sonn SK, SE J, Seo S, et al. Peroxiredoxin 3 deficiency induces cardiac hypertrophy and dysfunction by impaired mitochondrial quality control. *Redox Biol.* 2022;51:102275.
- [58] Kim J, Cheon H, Jeong YT, et al. Amyloidogenic peptide oligomer accumulation in autophagy-deficient  $\beta$  cells induces diabetes. *J Clin Invest.* 2014;125(8):3311–3324. DOI:10.1172/JCI69625
- [59] Kim KH, Jeong YT, Oh H, et al. Autophagy deficiency leads to protection from obesity and insulin resistance by inducing Fgf21 as a mitokine. *Nat Med.* 2013;19(1):83–92. DOI:10.1038/nm.3014